Int. Agrophysics, 2006, 20, 1-10

INTERNATIONAL
Agrophysics
www.ipan.lublin.pl/int-agrophysics

Investigations of plant infections by thermal vision and NIR imaging**

H.J. Hellebrand[1], W.B. Herppich[2], H. Beuche[1], K.-H. Dammer[3], M. Linke[2], and K. Flath[4]*

[1]Department of Technology Assessment and Substance Cycles
[2]Department of Horticultural Engineering
[3]Department of Engineering for Crop Production
Leibniz-Institute of Agricultural Engineering Potsdam-Bornim (ATB), Max-Eyth-Allee 100, D-14469 Potsdam, Germany
[4]Institute for Plant Protection in Field Crops and Grassland, Federal Authority and Federal Research Centre for Agriculture and Forestry, Station Kleinmachnow, Stahnsdorfer Damm 81, D-14532 Kleinmachnow, Germany

Received May 13, 2005; accepted July 8, 2005

A b s t r a c t. The successful applicability of thermal vision in horticulture was the starting point to launch a project in plant protection. Earlier studies proved the applicability of thermal vision for the assessment of freshness status and of microbial infestation by local temperature differences of plant parts. In recent laboratory experiments, studies were performed on the development of infestation of wheat plants which were infected by powdery mildew and by stripe rust. Fungi infections, which may cause variations of the surface temperature of plants, could be recognised by infrared cameras in the thermal range under laboratory conditions. Field studies revealed that pronounced natural temperature variations of several Kelvin within the crop canopy prevented the recognition of infected plants. Additionally, the comparatively low resolution of commercial thermal vision systems limited the detection chances of fungi-caused temperature variations within the plant canopy. Near infrared cameras fitted with band-pass filters showed different intensity distributions of the reflected radiation. The evaluation of the spectral intensity relations improved the differentiation.

K e y w o r d s: infrared imaging, transpiration, plant discrimination, fungi infections

INTRODUCTION

Remote recognition and evaluation of plants and plant products is usually based upon spectral signatures or image processing in the visible (VIS; approx. 0.4 to about 0.7 μm), near infrared (NIR; 0.7 to 3 μm), and middle infrared (MIR; 3 to 25 μm) wavelength ranges. Harmonic vibrations and combination vibrations of molecular parts (CH-, OH-, and NH-bonds) determine the line shape and spectral intensity distribution in the NIR range. Thus the contents of sugar, oil, protein, organic acids, and water in plants and other media are measured by NIR spectroscopy (Osborne and Fearn, 1986). To discriminate plants and to recognize plant stress and infections, differences in colour and shape are essential (geometry and morphology), and additionally to spectral information, shape evaluation by machine vision can be successful (Bennedsen and Peterson, 2005; Gerhards *et al*., 1993; Guyer *et al*., 1986 and 1993; Lillesand and Kiefer, 2000; Woebbecke *et al*., 1995a and 1995b). Furthermore, stressed and infected plants may show harmed function of the chloroplasts. In these cases, the chlorophyll fluorescence is the suitable method (Daley, 1995; Herppich, 2002; Von Willert *et al*., 1995). Plant stress and plant damage can be determined by chlorophyll fluorescence at plant conditions, where the human eye does not recognize anything. If stresses or infections of plants result in changes of surface temperatures due to their effects on metabolism *eg* microbial infections, nutrient stress, or transpiration *eg* infestations, drought stress, then the relevant plants can be detected by thermography (Inoue, 1990; Nilsson, 1995; Hellebrand *et al*., 2004). Plants with different transpiration rates have different surface temperatures as a result of the latent heat necessary for water evaporation. The temperature decreases when the heat, dissipated from the product for the transformation of water into vapour, exceeds energy influx from the surroundings and metabolic heat generation. The water status of leaves and fruits can influence the properties of the biological object. Furthermore, transpirational water

*Corresponding author's e-mail: jhellebrand@atb-potsdam.de
**The paper is published in the frame of activity of the Centre of Excellence AGROPHYSICS - Contract No. QLAM-2001-00428 sponsored by EU within the 5FP.

losses also depend on the type and state of plants or fruits (size, shape, skin properties, stage of development, *etc*), the temperature and humidity of the surrounding air, and on the airflow around and against the object.

Whereas the recognition of single plants, and so the differentiation between crops and weeds, is solved principally by means of grey or binary image processing, this method usually fails for high density crops. Only multispectral image processing has the potential to identify weed distributions on fields and to analyse areas with infested plants (Lillesand and Kiefer, 2000). The pixels of infrared cameras are intensity values ('grey levels') which are attributed to temperature (in °F, K or °C) or radiant flux densities (in W m^{-2}) by calibration. The intensity distribution is visualised by 'false colours'. Should it be possible to determine properties of the infestation as specific quantitative intensity distribution, then a simple control of plant protection machines could be derived using threshold algorithms in the image evaluation analysis.

Projects recently conducted at the ATB proved the applicability of thermography in horticulture: Air conditioning and air flow in storage houses (Geyer *et al*., 2004a and 2004b); Control and design of cold storage conditions; Classification of horticultural products regarding transpiration losses due to surface destruction during cleaning procedures; Evaluation of changes in turgor of sensitive horticultural products *eg* freshness of lettuce and other vegetables, and discrimination of varieties and ripening stages of fruits (Linke *et al*., 2000; 2001). It was possible to detect microbial infections by thermal vision during the rotting of peaches. There were diverging results in the tests of microbial infestations of vegetable greens. In some cases an increased transpiration was observed, whereas in other cases the transpiration did not change and thus thermal vision could not sense this type of infestation (Hellebrand *et al*., 2002). Because of these promising applications so far, a new project was launched to evaluate the chances of infrared imaging in plant protection.

The first questions which had to be tackled, were: Is it possible to differentiate healthy and infected plants by currently available NIR and MIR cameras? Are there recognizable differences between crops and weeds in infrared images? There are numerous papers which show the applicability of VIS and NIR spectroscopic methods for the detection of plant infections and weed (Amon and Schneider, 1993; Brown *et al*., 1994; Woebbecke *et al*., 1995b). Near infrared measures the reflected radiation, *ie* the difference between the radiation incident on a plant and that absorbed and transmitted by the upper tissue layers. For this reason, the reflected NIR radiation contains information up to a penetration depth of about 5 to 10 μm. Water molecules cause absorption bands in the wavelength ranges of approximately 1.1, 1.4, 1.9, 2.6, and 6.2 μm and longer wavelengths. The absorption rises with increasing wavelength. Because the structure of surface tissue cells and their soluble contents influence the NIR reflection, differences in the reflectance are expected between different parts of one plant as well as between various plants. Thermography is the temperature visualisation of the superposition of self-radiation of the object under consideration and the reflection of heat sources at the object's surface. If a pathogen infection affects the transpiration rate of plants, thermography should enable this infection to be recognized.

MATERIALS AND METHODS

Plants and experiments

To test the principal suitability of thermography for the recognition of plant infection, the responses of wheat plants (*Triticum aestivum*, variety 'Kanzler') to an infection by powdery mildew (*Blumeria* [syn. *Erysiphe*] *graminis* DC. f. sp. *tritici* March.) was analysed in laboratory experiments in 2002 and 2003. In 2004, laboratory studies were performed on wheat plants (Kanzler and a wheat breading line) infected by stripe rust (*Puccinia striiformis* West.). In 2005, a VIS NIR spectrometer was available and spectra could be included in the evaluation. From 2003 on, additional measurements with a NIR camera were possible. Since 2003, tractor mounted NIR and MIR cameras could be used for field trials. The cameras, fixed at the roof of the tractor, had a height of about 2.5 m above the ground and the optical axis was *ca*. 30° to the perpendicular axis. For these investigations on parallel stripes of 3 m width, wheat plants were sprayed with a dosage equivalent of 1 l ha^{-1} of the fungicide JuwelTop® while on the remaining area plants were not treated (Fig. 1). These field trials were a part of a ring test, the aim of which was to evaluate the principal potential of different commercially available equipment for the recognition of infections and infestation state of plants. One condition for the suitability of the selected remote sensing systems was that the measurements could be performed on the go with a speed at which tractor is operating during spraying of fields (1.5-3 m s^{-1}). Results, presented here, concern infrared imaging. The first task was to analyse, in laboratory studies, if infected plants show effects which could be visualised by infrared imaging. The next question which had to be tackled was the evaluation of chances and difficulties of tractor based infrared imaging. And thirdly, it was to find out if infrared imaging can be a part of a sensor fusion system.

In 2003, four test runs were performed at the experimental field shown in Fig. 1, in the period between June 11 and July 10, and in 2004, when seven test runs occurred between May 25 and July 07. Because of the dry weather (128 mm total precipitation from May to July), the infestation level was very low in 2003. In 2004, the precipitation was 218 mm in the same period from May to July, and thus a higher level of infestation was rated on the non-sprayed

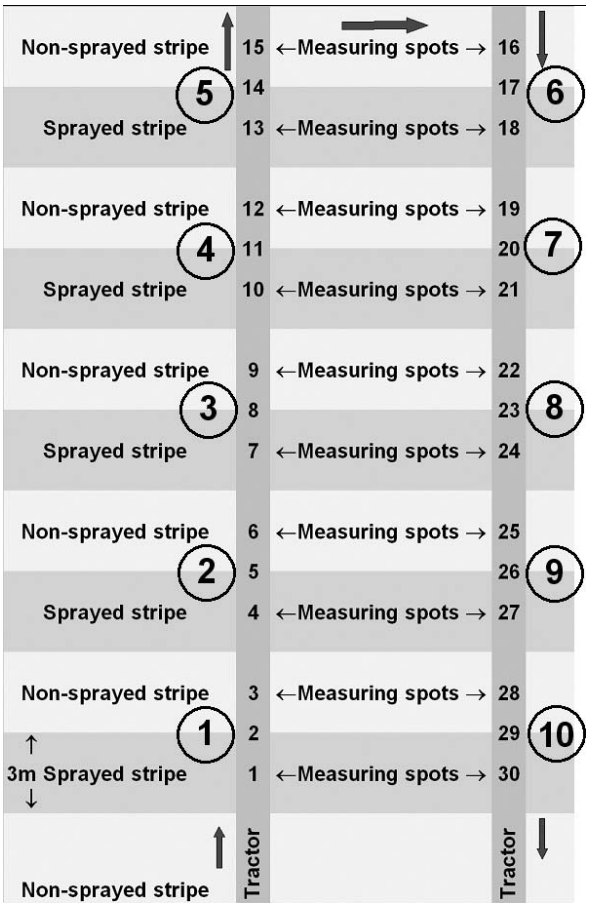

Fig. 1. Schematic of the experimental field. Circled numbers correspond to the measuring plots, given in Figs 8 and 9. At each plot, there were three measuring spots (sprayed area, borderline sprayed/non-sprayed, and non-sprayed area). Three images (VIS, NIR and MIR) were taken at each measuring spot. Plant density, average plant height, temperature (20 cm below and above plant tips), humidity (20 cm below and above plant tips) and wind speed was measured at each measuring plot 1 to 10 (Fig. 9; borderline between sprayed and non-sprayed stripes).

parts of the field. Pot experiments with infected and healthy wheat plants were performed in laboratory studies. The laboratory was air conditioned and thermal insulted in order to avoid disturbing reflections from heat radiation sources like heating elements and other hot devices.

Cameras and spectral evaluation

For the measurement of ambient temperatures (*eg* -20 to +100°C), thermographic cameras use middle infrared (MIR) in the wavelength band from about 8 to13 μm (Table 1) which includes the radiation maximum of a black body at a temperature of 300 K. The infrared thermography camera Varioscan™ 3021-ST (Jenoptik Technologie GmbH) with Stirling cooled MCT-Sensor was applied in laboratory experiments. The advantage of this scanning system is its higher sensitivity and resolution (Table 1). Because of its low frame rate of 1.1 s^{-1}, the system can be utilised for static scenes only. Routine images along the measuring path of the field with sprayed stripes were gained by the FPA-camera (Focal Plane Array) with unchilled micro-bolometer ThermaCAM® SC 500 (FLIR Systems GmbH). This camera has a high frame rate of up to 50 s^{-1} and thus is suitable for dynamic scenes. The ThermaCAM SC 500 was mounted at the tractor together with the ALPHA NIR™ camera. The FPA-camera ALPHA NIR™ (Indigo Systems Corporation, now FLIR Systems) with high sensitive InGaAs-Sensor (Indium Gallium Arsenide) in the wavelength band of 0.9-1.7 μm has a frame rate of 30 s^{-1} and is suitable for dynamic applications, too. A handier FPA-camera ThermaCAM 545 was taken for manual documentation of selected scenes. Optical images were gained with a conventional digital camera.

Alpha^{TM} wavelength band-pass filters (LASER COMPONENTS GmbH; 150 nm Full Width at Half Maximum - FWHM) and central wavelengths of 1 000, 1 075, 1 175 and 1 420 nm were attached to the NIR camera by a self-made device during laboratory studies. Spectra in the VIS and NIR range were measured using a spectrometer system based on the modules MMS1 NIR enhanced (400-1100 nm) and MMS NIR 1.7tc (900-1 700 nm), Carl Zeiss Jena GmbH, Spektralsensorik. Halogen bulbs served as light source and quartz glass fibre were used for light transmission. From healthy and infected plants, ten spectra each were taken from the upper and the lower sides of the leaf. The reflectance measurements were internally calibrated. Hence, reflectance is given in relative units. Because of internal calibration, all spectra are comparable with each other and can be evaluated without correction factors.

Infrared temperature measuring errors

Several error sources limit the accuracy of infrared temperature determination. The radiant energy flux, measured by IR cameras, depends proportionally on the emissivity and – to the power of four – on the temperature (Stefan-Boltzmann law). Therefore, the emissivity of the object in the interesting waveband should be known to convert radiation data into temperature. In practice, a constant emissivity of about $\varepsilon = 0.95$ is applied for all objects of the image, since most of the surfaces of biological objects show emissivities of 0.96 ± 0.03 (Hellebrand *et al*., 2002). These thermal measurements, utilising constant emissivity settings without local corrections, are called apparent temperatures. The deviations in emissivity have a minor influence on the image error patterns in case the temperature change in time of one object is considered or the temperature of similar plant parts are evaluated.

T a b l e 1. Selected features of IR imaging cameras

Specification	Varioscan™ 3021-ST	ThermaCAM SC 500	ThermaCAM 545	ALPHA NIR™
Spectral range	8 to 12 μm	7.5 to 13 μm	7.5 to 13 μm	0.9 to 1.7 μm
Measuring range	-40 to +1200°C	-20 to +500°C optional to +2000°C	-20 to +350°C optional to +1000°C	$2x10^{-9}$ to <1 W cm^{-2}
Resolution	0.03 K at 30°C	0.07 K at 30°C	0.1 K at 30°C	10^{10} photons cm^{-2} s^{-1}
Absolute measurement accuracy	< ± 2K, ±1%	< ± 2K, ±2%	< ± 2K, ±2%	Linear dynamic range: 66 dB Total dynamic range: 69 dB
Spatial resolution	1.3 mrad	1.3 mrad	1.5 mrad	1.2 or opt. 0.6 mrad
Sensor type	Scanner, HgCdTe, Stirling cooled	FPA, uncooled microbolometer	FPA, uncooled microbolometer	FPA, InGaAs, thermoelectric stabilization
Image size	360h x 240v pixel	320h x 240v pixel	320h x 240v pixel	320h x 256v pixel
Frame rate	1.1 Hz	50/60 Hz non-interlaced	50/60 Hz non-interlaced	30 Hz

Sources:
http://www.jenoptik-los.de/data/downloads/157/Varioscan_Prospekt_de.pdf
http://tssi.com.my/img/flir/Brochures/545.pdf
http://www.indigosystems.com/product/alphanir_specs.html
http://www.flir.com.hk/Download/Brochures/SC500_E.pdf
http://www.flir.com.hk/Download/Brochures/SC3000_E.pdf
http://www.flirthermography.co.uk/images/PDF-ENG/Newsletter%202%20EN.pdf

The thermal electromagnetic radiation of a body is a superposition of direct radiation and of diffuse radiation. Due to this, additional errors may occur in evaluating thermal images. The radiation intensity depends on the angle between measuring direction and the normal vector of the surface under consideration. If the surface emitted thermal radiation with the intensity distribution according Lambert's (cosine) law, then even an arbitrary shaped body would give equal temperatures at all pixels at the projection on the measuring sensor plane. Because of the superposition of direct and diffuse radiation, the surface parts with strongly deviating normal vectors from the measuring direction appear to be cooler. The share of direct radiation of water, the main component of plants, fruits, and vegetables, depends on the thickness of the water layer (Haußecker, 1996). Those parts of fruit surfaces oriented nearly perpendicular to the sensor plane of the camera will be measured incorrectly. This effect is visible in thermal images of spherical shaped fruit, *eg* apples or tomatoes. The temperature at the outer circumference seems to be lower than from the centre of the fruit. Furthermore, thin laminar air layers superpose this effect. Across these air layers we find the temperature gradient caused by heat exchange between objects under consideration.

There are additional sources of errors in thermal imaging, resulting from ambient conditions like humidity and airflow variations near the object, superposition of thermal radiation of other objects due to reflection at the measured surface. Then a systematic error may be caused by the model (software) used for temperature calculation, if parameters like humidity, distance, absorption or others cannot be adapted to the real conditions during the measurements. For the evaluation of plants, fruits and vegetables, usually all of these errors can be neglected, if products are compared within one image or at constant ambient conditions and grouped in rough clusters only.

RESULTS AND DISCUSSION

NIR measurements

Spectral bands with and without water absorption are in the NIR range (Fig. 2). Infection by fungi and other microorganisms can affect the surface structure, *eg* drying and different kinds of changes caused by cuticula decomposing enzymes or the formation of mycelia. Therefore, spectra of healthy and infected leaves were investigated and infrared images of healthy and infected plants were taken by the NIR camera with mounted band-pass filters which had

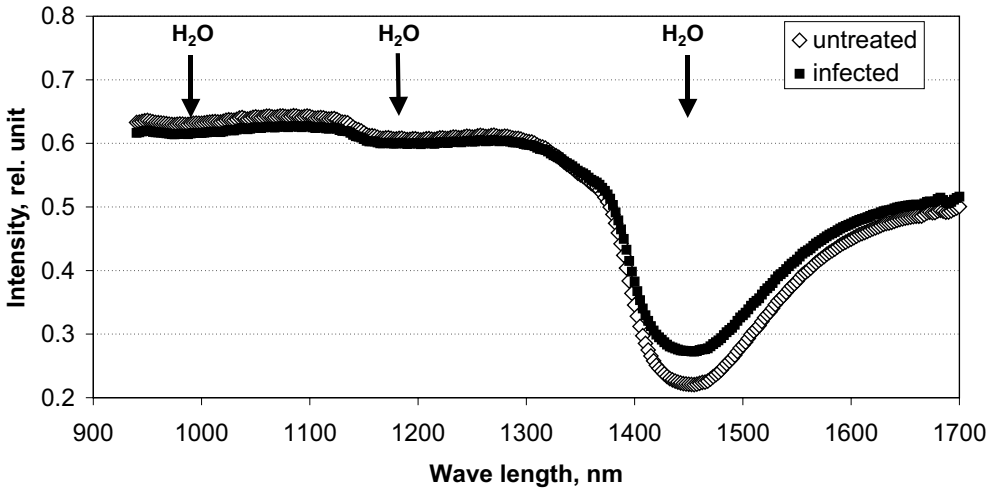

Fig. 2. NIR reflection spectra of healthy wheat plants (*Triticum aestivum*, variety Kanzler) and of plants infected by stripe rust (*Puccinia striiformis* West.). Each given spectrum is the mean of 20 individual spectra. Arrows indicate H_2O absorption wave bands.

transmission ranges inside and outside the water absorption band (around 1.4 μm). With this approach, the water containing surface tissues can be evaluated by image processing, whereas thermography assesses the transpiration rate of the plants.

Outside the water absorption band, the NIR reflection of infected plants leaves slightly decreased compared to that of healthy plants. In contrast, a slight increase was measured in the water absorption band for the infected leaves (Fig. 2). The differences between healthy and infected plants are marginal and the standard deviations of the means overlap nearly totally. Due to these small differences, efficient discrimination is not possible. Because the intensity changes are opposite inside and outside the water absorption band, the ratio of intensities improves the chances for differentiation. Healthy plant leaves show a spectral intensity ratio (1 070-1 100 to 1 435-1 465 nm) of 5.78 ($\sigma = 0.35$ with a sample size of 240). Plant leaves infected by stripe rust have a spectral intensity ratio of 4.68 ($\sigma = 0.83$ with a sample size of 240).

Healthy plants should show higher reflectance (*ie* being 'bright') in NIR images, gained band-pass filter 1070 ± 75 nm, and have lower intensity (*ie* being 'darker') with band-pass filter in the water absorption band (1420 ± 75 nm). In fact, the NIR images at wavelengths of 1 075 and 1 420 nm differ from each other (Fig. 3). In the water absorption band (1420 nm), most of the plant parts are darker than with the band-pass filter of 1 075 nm. This difference in the images can be intensified by image processing, *eg* conversion into binary images (Fig. 4) or ratio of pixels and subtraction of pixels, respectively (Fig. 5). Subtraction or division

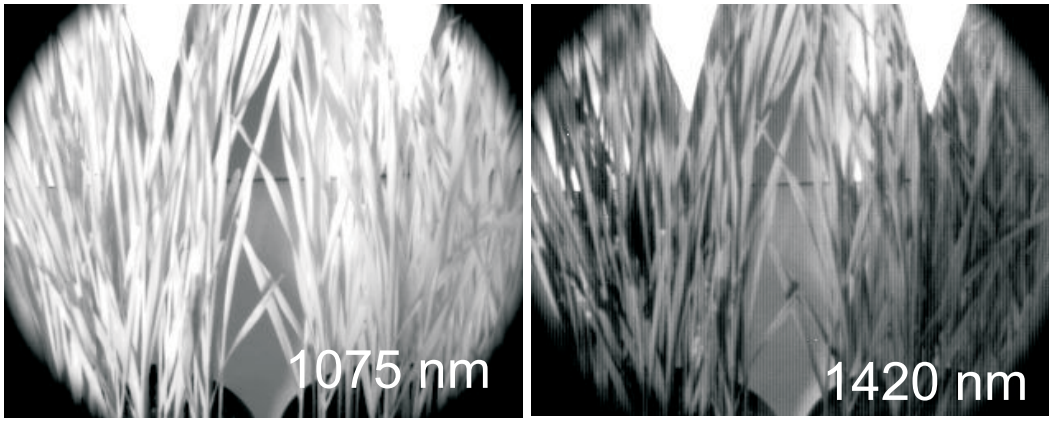

Fig. 3. NIR images of wheat plants (*Triticum aestivum*, variety Kanzler) infected by powdery mildew (*Blumeria* [syn. *Erysiphe*] *graminis* DC. f. sp. *tritici* March.; left pot*)* and of healthy wheat plants (right pot). NIR 1075: Image of NIR camera fitted with band-pass filter 1075 ± 75 nm, NIR 1420: Image of NIR camera fitted with band-pass filter 1420 ± 75 nm.

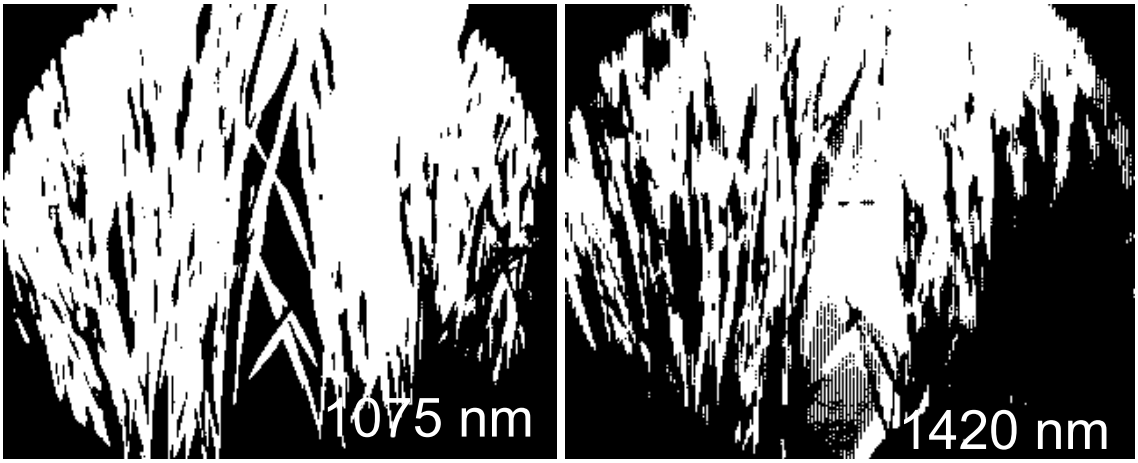

Fig. 4. Binary images of the NIR images with band-pass filters in Fig. 3. The threshold for conversion was set to 128.

improves the visibility of those image parts which show essential intensity differences in the two filter wave bands. Therefore, mainly plant parts are visible in Fig. 5, while other details are suppressed. In general, the differences between infected and healthy plants depend on the angle of image taking and changes during the course of infection. Thus suitable information for plant protection cannot be derived easily. A pixel processing of two or more identical NIR images with different wavelength ranges may provide a better solution for successful analyses because intensity ratios improve the discrimination potential in the NIR range (Sökefeld and Gerhards, 2004).

Thermographic measurements

In the case of stripe rust infection, the temperature differences between healthy and infected plants were nearly always below ±0.1 K. In contrast, powdery mildew infection clearly induced higher temperature changes. Usually, when the powdery mildew mycelia became visible, the temperature of plant leaves decreased. After a few days, the average temperature of these infected plant parts were 0.2 to 0.9 K lower than those of healthy plants (Fig. 6). In some trials, the temperature distribution across the foliage developed differently during the course of the infection. The temperature of later grown leaves of infected plants, which

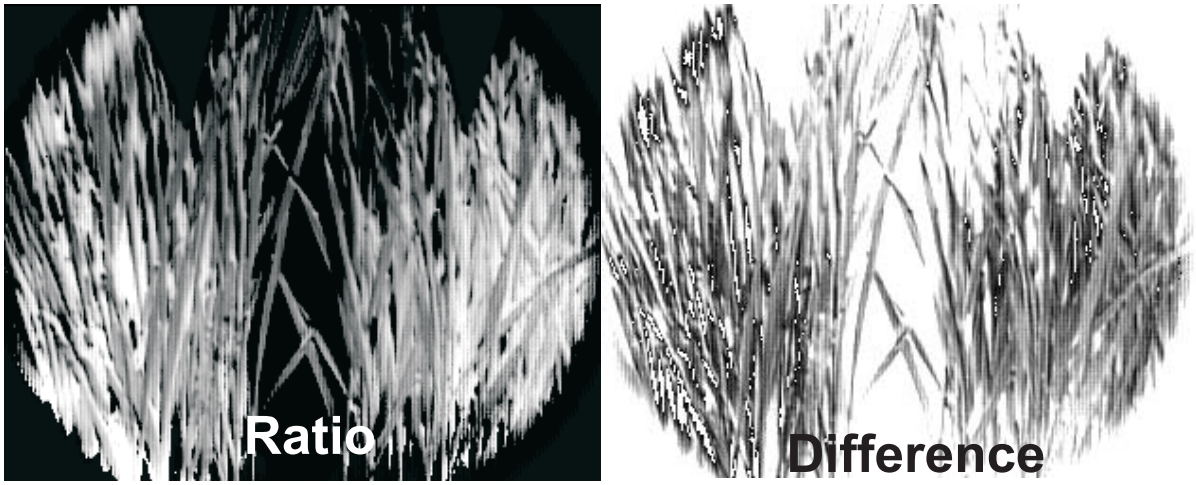

Fig. 5. Ratio and difference of the NIR images obtained with band-pass filters (Fig. 3). The ratio of pixels and transformation into the image intensity levels was performed by a custom-made software. The difference was taken by commercial software. Depending on software parameters chosen, each image may appear as inverted version.

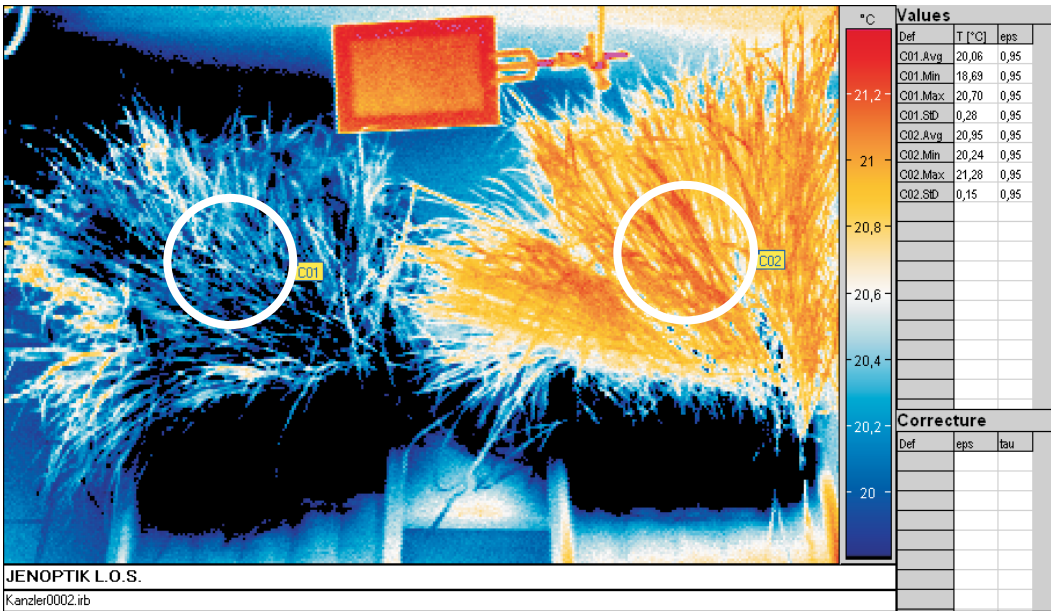

Fig. 6. Thermal image of wheat plants *(Triticum aestivum*, variety Kanzler). T=22.5°C, RH=47%. Left plants are infected with powdery mildew (*Blumeria* [syn. *Erysiphe*] *graminis* DC. f. sp. *tritici* March.) and right plants are healthy. Temperature (°C) in left measuring circle C01: average 20.1; minimum 18.7; maximum 20.7; standard deviation 0.3. Temperature (°C) in right measuring circle C02: average 21.0; minimum 20.2; maximum 21.3; standard deviation 0.15.

looked healthy *ie* no fungi mycelia on leaves, increased and reached higher values relative to healthy plants. However, leaf temperature was always below the temperature of the ambient air (Fig. 7).

The instantaneous temperature of leaves and other plant parts is primarily determined by the balance between heat and energy influx from the surroundings and heat dissipation by transpiration. Usually, transpirational energy dissipation dominates the energy balance and, hence, the temperature of free standing plants (without consideration of external heat sources). The most likely explanation of the measured temperature characteristics is that the infection with powdery mildew results in an initial increase of the transpiration rate of infested plant surfaces, giving additional surface cooling. The growing mycelia, which have a very low evaporation resistance, may largely increase the total transpiration area. During later infection, the affected leaf parts will be damaged, the tissue dries and, therefore, the

Fig. 7. Visible wave-band (VIS) and thermal (MIR) images of wheat plants (*Triticum aestivum*, variety Kanzler) infected with powdery mildew (*Blumeria* [syn. *Erysiphe*] *graminis* DC. f. sp. *tritici* March.; left pot*)* and of healthy wheat plants (right pot), air temperature 24.1°C, relative humidity 52%.

transpiration of the infested parts will be largely reduced or even stops. It is to assume that infected leaves disturb the water status of the entire plant. This would explain why healthy parts of infested plant could have higher temperatures than leaves of healthy plants under the same environmental conditions (Fig. 7). As a result, this largely complicates the recognition of plant infections, as different effects occur at different states of infection.

The field trials indicated a second difficulty for the application of thermal vision. It is nearly hopeless to get information for plant protection by simple image evaluation methods like average values of temperature of the measuring area, or minima, maxima, and standard deviations of the temperature pixels of the measuring area. The reason for this problem is a natural temperature variation of several Kelvin occurring within a plant canopy (Figs 8 and 9). According to the infrared images (mean value), the adjoining stripes at measuring plot 2 had a temperature difference of 2 K. The temperature variation within one image may exceed 10 K depending on the position of the sun, plant density, soil type *etc*. Dry soil is usually hotter than plants. Thus, direct solar irradiation is a major factor causing temperature variations within thermal images (Fig. 8 with measuring spots 4, 5, and 6; Fig. 1). The influence of direct sunlight can be recognised from Fig. 9A and Fig. 9B. On a sunny day (Fig. 9A), the differences between air temperature and plant temperature are higher then on a cloudy and cooler day (Fig. 9B). The natural variations are the result of pronounced shadowing effects due to different plant height and plant density, and may be considerably higher than any changes caused by infections. Additionally, the measured temperature depends on the angle of the camera relative to the direction of the solar irradiation. Furthermore, the heterogeneity of air motion (wind and buoyancy) within the canopy affects convection and may lead to different transpiration rates, and hence, to different cooling rates.

The presented results indicate that thermography certainly has the potential to recognize infected plants. However, as the natural temperature variations within the crops and within thermal images are considerably higher than those due to infection effects, information for plant protection cannot be obtained from thermal images with only 320x240 pixels, standing for hundreds of wheat plants. Only the detailed evaluation of each plant at images with much higher resolution bears the chance to detect infection caused temperature changes. Therefore, currently available commercial thermal vision systems cannot solve this task as tractor mounted stand-alone solution. Nevertheless, the question whether a combination of cameras with different wave ranges (VIS, NIR) or with different principles (fluorescence) can improve the reliability and effectiveness of the remote evaluation is still unanswered.

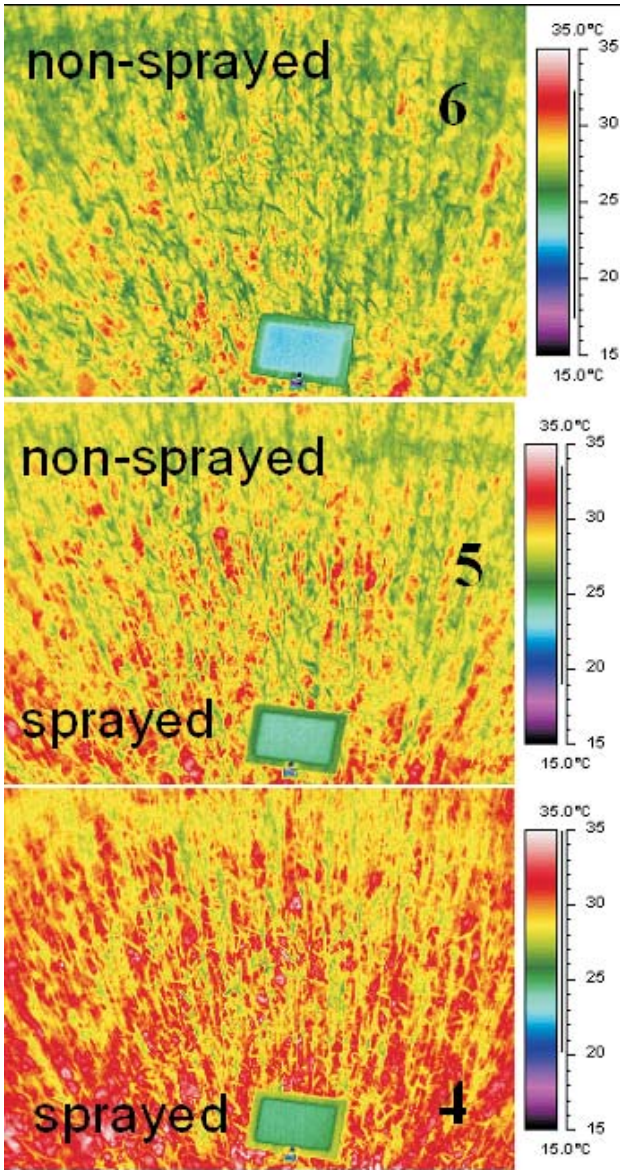

Fig. 8. Thermal images of winter wheat of the experimental field at measuring plot 2 (c.f. Fig. 9) with non-sprayed area (upper image), borderline between sprayed and non-sprayed stripe (middle image), and sprayed stripe (lower image). The colours of the images refer to apparent temperatures with an emissivity of 0.95. The lower part of the images show a plate with calibrated emissivity of 0.93. Measuring conditions: June 11, 2003, 1.45 p.m., full sunshine, air temperature within plant canopy 32.5°C (measured 20 cm below plant tip), average crop height 57 cm, relative humidity 42.4%, (measured 20 cm below plant tip), air speed approx. 5 m s^{-1}. Non-sprayed spot: minimum temperature 25.2°C; maximum temperature 31.7°C; average 27.7°C. Stripe sprayed: minimum temperature 26.1°C; maximum temperature 36.1°C; average 29.7°C.

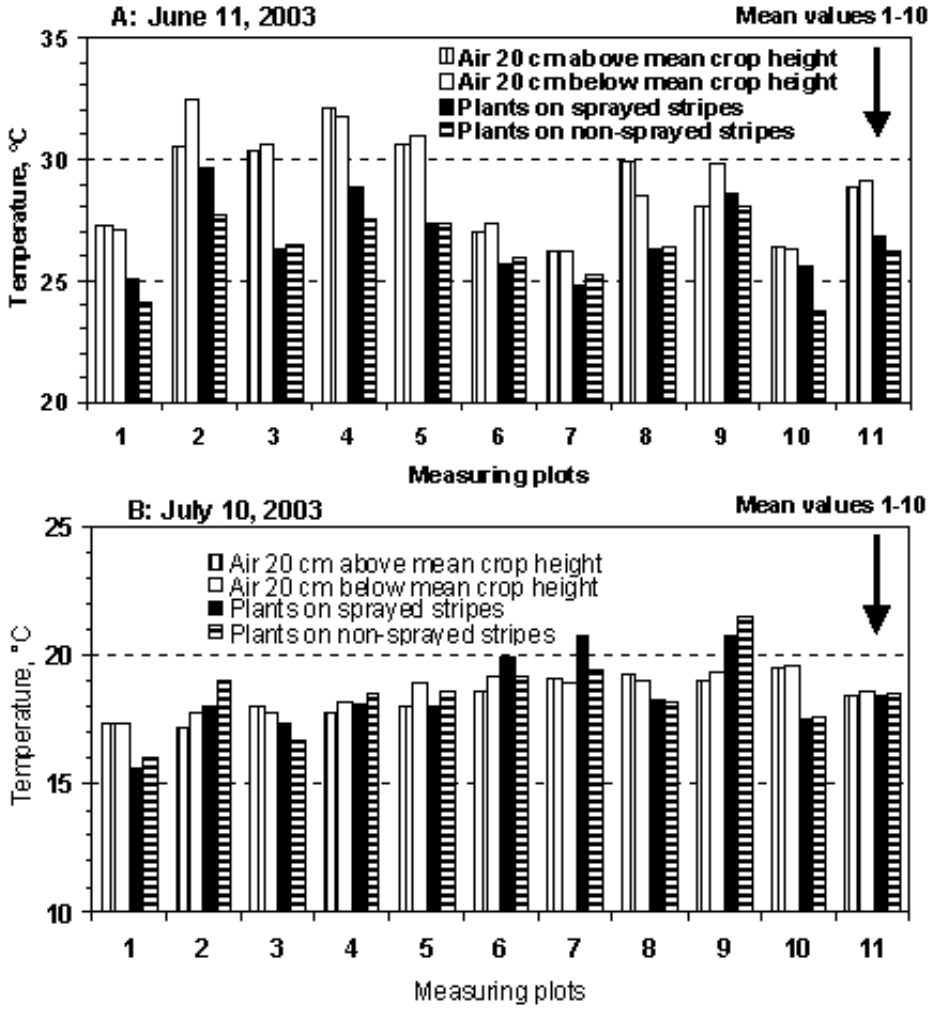

Fig. 9. Air temperatures, temperatures of fungicide-treated winter wheat plants and of non-sprayed plants growing at adjoining stripes. The plant temperature was measured by thermography, air temperature and relative humidity was measured 20 cm below and 20 cm above the average plant tip of the corresponding measuring spot. A: Measurement on June 11, 2003, 1.00-4.00 p.m.; variability between measuring spots: sunny day (few clouds, sunshine between *ca*. 50 and 100%), air temperature 26.2-32.5°C, relative humidity 42.4-66.2%, air speed 1-9 m s^{-1}. B: Measurement on July 10, 2003, 10.10-11.30 a.m.; variability between measuring spots: cloudy day (sunshine between *ca*. 0 and 25%), air temperature 17.2-19.9°C, relative humidity 53.8-66.5%, air speed 3- 9 m s^{-1}.

Perspective

Multi-spectral images in the VIS/NIR range are not a serious technological obstacle nowadays. This wave range can be tackled with appropriate lenses and ray dividers. Weed mapping by means of the combination of VIS and NIR image processing can serve as an example (Sökefeld and Gerhards, 2004). Suitable conditions must be chosen for synchronic online imaging in the thermal and NIR range, in order to obtain comparable measuring spots for both wave bands. Since different materials are utilised for the optical part (NIR: glass and MIR: Germanium), joint lens and joint ray dividers are not available at present. If NIR and MIR cameras should be combined for online detection of infestation, only the intensity of overlapping image parts can be used. Additionally, the NIR image should be represented by images, processed for several wave bands, because the directly measured NIR intensity distribution has lower potential for plant discrimination.

CONCLUSIONS

1. It could be shown in laboratory studies that thermography has the potential to recognize fungi infections of plants. However, as the natural temperature variations within the crops are higher than those due to infection effects, information for plant protection cannot be obtained online, based on simplified image evaluation of images with 10^4 to 10^5 pixels as provided by currently available commercial thermal vision systems. More sophisticated studies are necessary to utilise the thermal information in sensor fusion systems.

2. A routine application of thermal imaging systems in plant protection would reach its limits very quickly. Not only the costs of these systems are still relatively high, but also the possibilities of use are restricted due to fluctuations in temperatures and humidity inside the crop canopy across the field. Local temperature variations due to sunshine and shadow effects prevent the discrimination of plants with the smaller temperature changes caused by infections. Thermal imaging as remote temperature sensing technology provides numerous, very suitable possibilities of use for scientific studies and in other areas with controlled air conditioning. When interpreting the results, the interrelation between the produce and its environment must always be taken into account.

3. In combination with suitable band-pass filters, near infrared imaging can visualise effects of water within surface tissues of plants. Since wide-band NIR imaging has a low potential for plant discrimination, imaging applications in plant protection should take advantage of processing of several wave bands in the NIR and VIS range.

REFERENCES

Amon H. and Schneider T., 1993. Anwendung spektraler Signaturen von Pflanzenbeständen für die Produktionstechnik im Pflanzenbau. Zeitschrift für Agrarinformatik, 3, 54-60.

Bennedsen B.S. and Peterson D.L., 2005. Performance of a system for apple surface identification in near-infrared images. Biosystems Eng., 90, 4, 419-431.

Brown R.B., Stechler J.-P.G.A., and Anderson G.W., 1994. Remote sensing for identification of weeds in no-till corn. Transactions of the ASAE, 37, 1, 297-302.

Daley P.F., 1995. Chlorophyll fluorescence analysis and imaging in plant stress and disease. Can. J. Plant Pathology, 17, 167-173.

Gerhards R., Nabout A., Sökefeld M., Kühbauch W., and Nour Eldin H.A., 1993. Automatische Erkennung von zehn Unkrautarten mit Hilfe digitaler Bildverarbeitung und Fouriertransformation J. Agronomy Crop Sci., 171, 321-328.

Geyer S., Gottschlalk K., Hellebrand H.J., Schlauderer R., and Beuche H., 2004a. Infrarot-Thermografie zur Klimasteuerung in einem Großkisten-Kartoffellager. Landtechnik, 59, 2, 96-97

Geyer S., Gottschlalk K., Hellebrand H.J., and Schlauderer R., 2004b. Application of thermal imaging measuring system to optimise the climate control of potato stores. AgEng Conf. Engineering the Future, Leuven, Belgium, 12-16.09.2004, Book of Abstracts, Part 2, 1066-1067.

Guyer D.E., Miles G.E., Gaultney L.D., and Schreiber M.M., 1993. Application of machine vision to shape analysis in leaf and plant identification. Transactions of the ASAE, 36, 1, 163-171.

Guyer D.E., Miles G.E., Schreiber M.M., Mitchell O.R., and Vanderbilt V.C., 1986. Machine vision and image processing for plant identification. Transactions of the ASAE, 29, 1500-1507.

Haußecker H., 1996. Messung und Simulation von kleinskaligen Austauschvorgängen an der Ozeanoberfläche mittels Thermographie. Ph.D. Thesis, Ruprecht-Karls-University, Heidelberg, http://klimt.iwr.uni-heidelberg.de/PublicFG/ProjectB/CFT/disshhaus/node20.html#transemiss.

Hellebrand H.J., Beuche H., and Linke M., 2002. Thermal imaging. A promising high-tec method in agriculture and horticulture. In: Physical Methods in Agriculture - Approach to Precision and Quality (Eds J.Blahovec and M. Kutílek), Kluwer Academic/Plenum Publishers, New York, 411-427.

Hellebrand H.J., Beuche H., Dammer K.H., and Flath K., 2004. Plant evaluation by NIR-imaging and thermal imaging. AgEng Conf. Engineering the Future, Leuven, Belgium, 12-16.09.2004, Book of Abstracts, Part 2, 946-947.

Herppich W. B., 2002. Chlorophyllfluoreszenzbildanalyse und Fluoreszenzspektralanalyse. Landtechnik, 57, 2, 98-99.

Inoue Y., 1990. Remote detection of physiological depression in crop plants with infrared thermal imagery. Japanese J. Crop Sci., 59, 4, 762-768.

Lillesand T. and Kiefer R., 2000. Remote Sensing and Image Interpretation. John Wiley and Sons Inc., New York.

Linke M., Beuche H., Geyer M., and Hellebrand H. J., 2000. Possibilities and limits of the use of thermography for the examination of horticultural products. Agrartechnische Forschung, 6, 6, 110-114.

Linke M., Herold B., and Hellebrand H.J., 2001. Thermographic studies of horticultural products. ASTEQ Final Plenary Meeting, Paris, 21/23 March, http://www.inapg.inra.fr/ens_rech/siab/asteq/abstract_Last%20Plenary.htm#THERMOGRAPHIC STUDIES.

Nilsson H.-E., 1995. Remote sensing and image analysis in plant pathology. Can. J. Plant Pathology, 17, 154-166.

Osborne B.G., Fearn T., 1986. Near Infrared Spectroscopy in Food Analysis. Longman Scientific and Technical, Harlow, Essex.

Sökefeld M. and Gerhards R., 2004. Automatische Unkrautkartierung mit digitaler Bildverarbeitung. Landtechnik, 59, 3, 154-155.

Von Willert D.J., Matyssek R., and Herppich W.B., 1995. Experimentelle Pflanzenökologie - Grundlagen und Anwendungen. Georg Thieme Verlag, Stuttgart.

Woebbecke D.M., Meyer G.E., Von Bargen K., and Mortensen D.A., 1995a. Color indices for weed identification under various soil, residue, and lighting conditions. Transactions of the ASAE, 38, 1, 259-269.

Woebbecke D.M., Meyer G.E., Von Bargen K., and Mortensen D.A., 1995b. Shape features for identifying young weeds using image analysis. Transactions of the ASAE, 38, 1, 271-281.